Blue-green spectral minimum correlates with oxyhemoglobin saturation *in vivo*

Kurt R. Denninghoff
University of Arizona
Department Emergency Medicine
and
Optical Sciences Center
Tucson, Arizona 85721

David A. Salyer
University of Arizona
Optical Sciences Center
Tucson, Arizona 85721

Sreenivasa Basavanthappa
University of Arizona
Department of Ophthalmology
Tucson, Arizona 85721

Robert I. Park
University of Arizona
Department of Ophthalmology
and
Optical Sciences Center
Tucson, Arizona 85721

Russell A. Chipman
University of Arizona
Optical Sciences Center
Tucson, Arizona 85721

Abstract. An imaging multi-spectral retinal oximeter with intravitrial illumination is used to perform the first *in vivo* test of the blue-green minima shift oximetry method (BGO) in swine eyes [K. R. Dennighoff, R. A. Chipman, and L. W. Hillman, *Opt. Lett.* **31**, 924–926 (2006); *J. Biomed. Opt.* **12**, 034020 (2007).] A fiber optic intravitreal illuminator inserted through the pars plana was coupled to a monochromator and used to illuminate the retina from an angle. A camera viewing through the cornea recorded a series of images at each wavelength. This intravitreal light source moves the specular vessel glint away from the center of the vessel and directly illuminates the fundus behind most blood vessels. These two conditions combine to provide accurate measurements of vessel and perivascular reflectance. Equations describing these different light paths are solved, and BGO is used to evaluate large retinal vessels. In order to test BGO calibration *in vivo*, data were acquired from swine with varied retinal arterial oxyhemoglobin saturations (60–100% saturation.). The arterial saturations determined using BGO to analyze the multispectral image sets showed excellent correlation with co-oximeter data (r^2=0.98, and residual error ±3.4% saturation) and are similar to results when hemoglobin and blood were analyzed using this technique. [DOI: 10.1117/1.3005390]

Keywords: biomedical optics; backscattering; image understanding; reflectometry; image evaluation.

Paper 08090R received Mar. 13, 2008; revised manuscript received Jun. 16, 2008; accepted for publication Aug. 4, 2008; published online Oct. 29, 2008.

1 Introduction

Measuring retinal vessel oxygen saturation levels could successfully detect relative hypoxia prior to vision-threatening complications, and therapy could be started early, potentially preventing disease progression. Retinal oximetry measurements may provide additional benefits by allowing the provider to give targeted therapy and to determine the response to treatments using the same technique.[1–3]

In an effort to address this need, retinal vessel oximetry was pioneered in 1963 by Hickham et al. prior to the development of the clinical pulse oximeter in the early 1970s.[4] Their system used a modified fundus camera that acquired dual quasi-monochromatic fundus photographs. Oxygen saturation was estimated by analyzing the optical density of the vessel images at each wavelength, and using oximetry equations based on the Lambert-Beer Law. This early system was used to demonstrate that the oxyhemoglobin saturations as well as retinal vessel reactivity seen in diabetic patients were abnormal.[4,5] Improvements to this fundus photography technique were made by Cohen and Laing[5] and Tiedeman et al.[6] The latter identified the influence of fundus reflectivity on these measurements and attempted to compensate for this and calibrate their measurements.[6] In addition to photographic retinal oximeters, systems have been developed that scan monochromatic beams across the retinal vasculature and collect the light that is scattered back out of the eye. The earliest scanning oximeter was developed by Delori,[7] and recent advancements have been made by Smith et al.[8] Schweitzer et al.[9] used a diffraction grating that measures the reflected optical spectrum of a retinal blood vessel in 2-nm increments from 510 to 586 nm. Schweitzer's group also published a method using three isobestic wavelengths and a measurement wavelength in this region to measure oxygen saturation in reflection.[10] Neff et al. applied a multispectral imager to retinal oximetry, illuminating with white light and capturing two or four images simultaneously through bandpass filters.[11] A similar two-wavelength retinal oximeter has been evaluated by Stefansson.[12] Central vessel glints, variations in fundus reflectivity, oxyhemoglobin intermediates, and red blood cell scattering significantly alter the measurement of optical signals in the eye and subsequent calculation of retinal blood oxygen saturations limiting the clinical use of these methods.[4,7,9,13–16] We have reported an invasive technique, intravitreal illumination, which allows for rejection of the cen-

Address all correspondence to: Kurt R. Denninghoff, University of Arizona, Department Emergency Medicine, Tucson, Arizona 85721. Tel: 520-626-1551; Fax: 520-626-2480; E-mail: kdenninghoff@aemrc.arizona.edu.

1083-3668/2008/13(5)/054059/9/$25.00 © 2008 SPIE

tral vessel glint and improved oximetry by displacing the vessel glint from the trans corneal solid collection angle in the swine eye.[17] We recently described the blue-green oximetry (BGO) technique, this approach takes advantage of the shift in the spectral minimum from around 470 to 510 nm as oxyhemoglobin increases from 0 to 100% of the hemoglobin present. BGO does not rely on the simplifications required by the methods used to date in retinal oximetry and is more accurate and more easily calibrated than the Lambert-Beer law–based methods when used in hemoglobin solutions or with intact red blood cells.[2,3] However, until now this new oximetry method has not been tested *in vivo*.

In the following, we use intravitrial illumination of the retina in swine to evaluate BGO *in vivo*.

2 Surgical Procedure and Animal Preparation

Intravitreal surgery was performed on four young (approximately five months old) female American Yorkshire domestic swine, and a series of experiments were performed using intravitreal illumination to measure the retinal blood oxygen saturation. The experimental methods procedure detailed below was performed on each swine. The experimental protocol was approved by the University of Arizona Institutional Animal Care & Use Committee.

The swine was administered a general anesthetic mixture consisting of air, nitrogen, oxygen, and isofluorane. Swan-Ganz catheters were placed through the femoral vein and artery to monitor blood pressure and arterial oxygen saturation (S_aO_2) and mixed venous oxygen saturation (S_vO_2). The first catheter tip was placed in the aorta just distal to the heart, and the second catheter tip was placed in the inferior vena cava just proximal to the heart. A peripheral oxygen-saturation monitor was also placed in the rectum of the swine, and a lid speculum was placed in the operative eye.

A 4-mm infusion cannulum was placed through the pars plana and sutured in place. The infusion cannulum was attached to a balanced salt solution gravity feed system to maintain intraocular pressure at ~14 cm of water. A contact vitrectomy lens (Bausch & Lomb, F36202.08, Rochester) was placed onto the cornea using an index-matching (refractive index: n_d=1.337) viscoelastic coupling agent.

3 Data Aquisition

Following the surgical preparation of the animal, light from a scanning monochromator (Oriel Spectral Luminator, Irvine) was coupled into a fiber optic intravitreal illuminator inserted through the pars plana into the vitreous illuminating the retina. The spectral resolution of the monochromator was ~10 nm. A 12-bit scientific-grade CCD camera (Hamamatsu Orca-AG) with a 3.3X macrozoom lens was used to image the retina. The peak wavelength of a 10-nm wavelength band was stepped from 420 to 700 nm, and an image of the target area was acquired at each illumination wavelength. All the retina were interrogated using the wavelengths 420, 430, 440, 460, 480, 490, 500, 510, 521, 532, 540, 545, 548, 552, 555, 558, 561, 565, 570, 575, 580, 590, 600, 615, 630, 645, 660, 680, and 700 nm. In two animals, additional wavelengths in the blue-green region were 475, 488, 506, and 514 nm. In order to minimize the 2–17% vessel-diameter change across the cardiac cycle,[18–20] each camera exposure was triggered using a cardiac monitor (Digicare Life Windows, Boynton Beach). By minimizing the effect of vessel pulsation, the associated change in optical path length during the cardiac cycle should also be minimized. Some studies indicate that systemic blood oxygen saturation can vary with cardiac cycle; also this effect is avoided by capturing spectral images at the same point in the cardiac cycle.[21] Finally, exposure time was adjusted to <40 ms (~1/25 of the cardiac cycle) in an attempt to minimize the blood vessel size variation during exposure.

The multispectral image sets were obtained over a 5 ×5 mm region of the illuminated fundus containing a selected vein/artery pair. A dark image (obtained with the shutter closed) was subtracted from each image on acquisition to correct for dark current and external light sources.

The measurement series began by setting the inspired respiration mixture to 100% oxygen, 0% medical-grade air. The animal was allowed to stabilize for 8 min and a multispectral retinal image set was acquired. The oxyhemoglobin saturation (SO_2), blood partial pressure of oxygen (PO_2), blood partial pressure of carbon dioxide (PCO_2), pH, and hematocrit were measured from small blood samples collected from the two Swan-Ganz catheters using an ISTAT Personal Clinical Analyzer (Heska Corporation). The measurement cycle (8-min stabilization, spectral data acquisition, and blood gas analysis) was repeated at 10% decrements, until a pulse oximeter read ~50%.

4 Data Calibration and Analysis

The data were calibrated for the spectral distribution of our illuminator by measuring the output port of an integrating sphere illuminated with the fiber optic illuminator. Then, the multispectral images were normalized by dividing the image intensities by this calibration data set. The inner wall of the integrating sphere is coated with Spectralon®, a common calibration standard.[22] This procedure ensured accurate pig's eye spectral reflectivity by minimizing any spectral power variations from the illumination system or the detector system.

The fundus multispectral image sets were registered to correct for eye motion during data collection, and images were aligned to within a fraction of a pixel using a bicubic spline interpolation in conjunction with a maximum mutual information merit function algorithm.[23]

5 Oxygen Saturation Calibration Standard

Absolute calibration of the retinal arterial oxyhemoglobin saturation ($S_{ra}O_2$) measurement relies on the assumption that large arterial oxygen saturation values are constant throughout the body and that the SO_2 in the aorta will be the same as the $S_{ra}O_2$.[24,25] This assumption is supported by the observation that the oxygen uptake from a vessel is based on the surface area-to-volume ratio and the retinal arterial vessels that we analyzed are all much larger than the capillaries where oxygen exchange primarily occurs.

6 Light Path Analysis

The multispectral retinal images were analyzed to determine the spectral reflectivity of the retina, the spectrum of scattering from blood vessels, the transmission of blood vessels, and the level of integrated scatter within the globe. These light

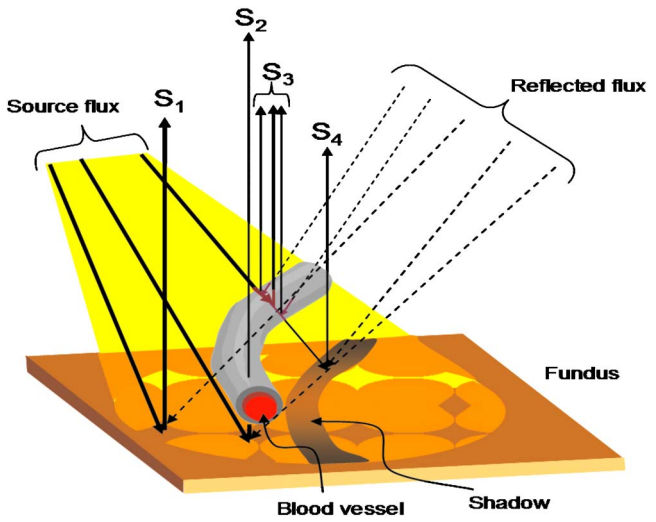

Fig. 1 Light paths in intravitrial illumination swine experiments. Specular reflections from the vessel wall and other structures are removed from the collection path by illuminating the retina from an angle. The perivascular retinal reflectance (S_1), single-pass reflectance from the retina through the vessel to the detector (S_2), the light scattered from the vessel wall and the vessel contents (S_3), and the vessel shadow (S_4) remain in the collection angle. The source flux (Ψ) is from the intravitrial fiberoptic light source, and the reflected flux (Ψ_r) shown is the scattered light from throughout the globe that reflects back onto the illuminated vessel and perivascular region.

fluxes were then applied to evaluate the oxygen saturation of a large artery and vein using BGO. Our initial motivation was to obtain the single-pass scattered light spectrum through vessels by (*i*) illuminating behind the vessels to provide a strong single-pass signal and (*ii*) move the vessel glint to the side of the vessel to minimize its interference with the transmitted signal. In the process of this experiment, we learned the significance of the light scattered from the blood column.

Figure 1 shows the set of light paths associated with these intravitreal illumination experiments. The source flux from the light pipe illuminates the fundus from the side, displacing reflected glints from the center of the vessel image well to the side of the vessel. The iris established the solid angle of the flux collected from the fundus. This method simplifies the collected flux from the vessels. Let Ψ be the flux incident on a point of interest in the fundus from the light pipe. The globe is also full of singly and multiply scattered light, similar to the inside of an integrating sphere. Let Ψ_r be the scattered flux incident on our point of interest.[17]

Four sets of ray paths are analyzed in our method. First the flux from the illuminated fundus S_1 is given by

$$S_1 = R_r(\Psi + \Psi_r), \tag{1}$$

where R_r is the spectral response of the light reflected from the avascular retina into the collection angle through the vitrious, lens, aqueous humor, cornea, and light collection system. The spectral dependence, such as the wavelength (λ) in $R_r(\lambda)$ has been suppressed from all expressions. When the camera collects light from blood vessels, two ray paths are significant. The flux S_2 from illumination behind the vessel that transmits through the vessel in single pass is

$$S_2 = R_r(\Psi + \Psi_r)T_sT_a. \tag{2}$$

The illumination behind the vessel comes both from the illumination system, Ψ, and from the multiply scattered light within the globe, Ψ_r. T_s is the fraction of the light that is not scattered out of the collection angle by blood in the vessel, the vessel wall, and other structures, and T_a is the fraction of the light that is not absorbed by the blood in the vessel, the vessel wall, and other structures. The light scattered from the vessel S_3 is related to the incident flux

$$S_3 = \Theta(\Psi + \Psi_r) \tag{3}$$

by Θ, the portion of the total incident flux that is scattered from the blood in the vessel, the vessel wall, and other structures into the collection angle. Thus, the total flux reflected from or through the center of the vessel into the collection angle, R_v, is

$$R_v = S_2 + S_3, \tag{4}$$

the sum of the transmitted and scattered components.

Finally, side illumination produces distinct vessel shadows in the retinal images, clearly displaced from the vessels. The flux collected from the vessel shadows S_4 is

$$S_4 = R_r\Psi(T_sT_a + \Psi_r). \tag{5}$$

This shadow is the result of the interaction of the scattered and transmitted light, the retinal reflectivity, and the power terms.

These equations, despite being approximations, provide insight into the underlying scattering processes as follows. The ratio of the vessel flux to the adjacent avascular fundus reflectance is

$$\frac{R_v}{S_1} = \frac{R_r(\Psi + \Psi_r)T_sT_a + \Theta(\Psi + \Psi_r)}{R_r(\Psi + \Psi_r)} = T_sT_a\frac{\Theta}{R_r}. \tag{6}$$

Equation (6) is independent of the flux terms, providing a solution expressed in transmission and scatter coefficients.

We have approximately determined T_sT_a from another experiment measuring the forward transmission of light through a 100-μm flow cell in a spectrophotometer.[3] The effective path length near the center of 130-μm cylindrical vein is similar in length to the flow cell. The blood hemoglobin concentration, effective path length, and oxyhemoglobin saturation were set close to the expected values for the swine eye, and the data used to approximate T_sT_a.[3] The spectrophotometer values of T_sT_a were compared to the measured value of R_v/S_1 at each wavelength, recognizing that this approximation neglects scattering and absorption by vessel walls.[3] We found the following relation held,

$$\frac{R_v}{S_1(130\text{-}\mu\text{m swine vein})} - (T_sT_a)(\text{spectrophotometer}) \approx \frac{\Theta}{R_r}. \tag{7}$$

The value of T_sT_a was $<2\%$ of the total Θ/R_r at all wavelengths tested from 450–700 nm, demonstrating that, for the wavelengths and the angle of incidence used in these swine,

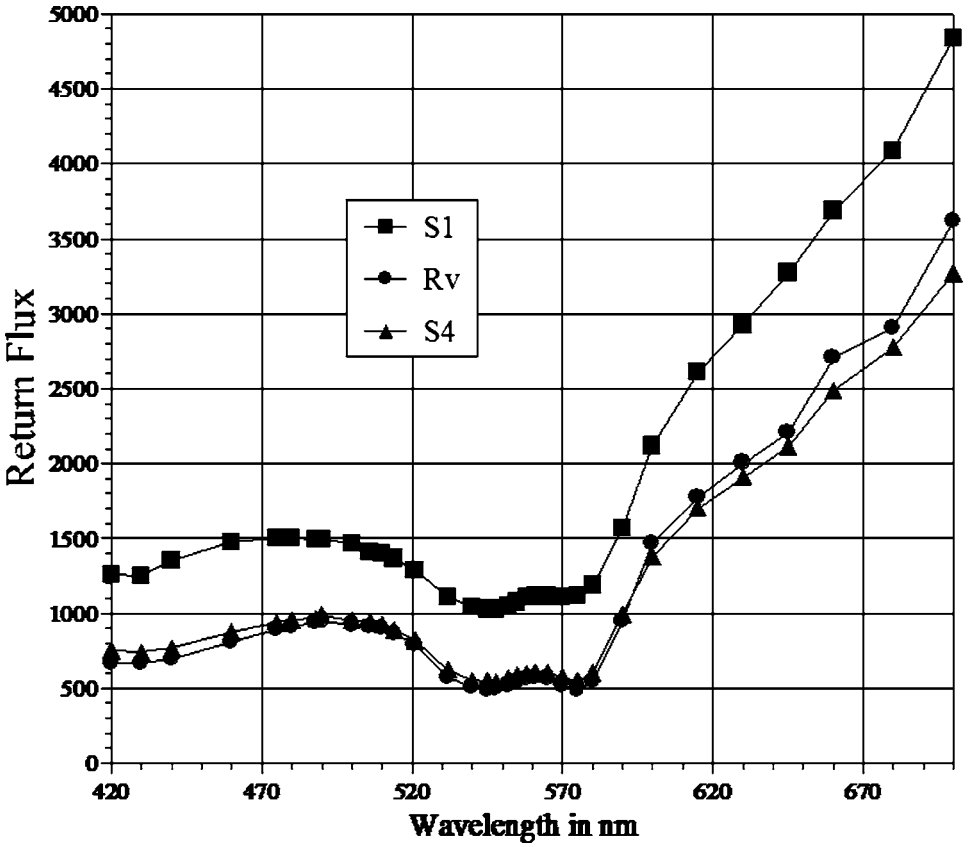

Fig. 2 The spectra of the measured components, S_1, R_v, and S_4 from a retinal vein are shown here. Each spectrum is a complex combination of the interaction of the source flux Ψ and the reflected flux Ψ_r with a specific region of the retinal anatomy. These signals are similar to the retinal reflectance spectra reported by others.[14]

the assumption that $\Theta/R_r \gg T_s T_a$ is reasonable. Thus, the approximation

$$\frac{R_v}{S_1} \approx \frac{\Theta}{R_r} \tag{8}$$

is valid. Equation (8) is useful because it is a ratio involving transmission and reflectance without any absolute flux terms and is relatively easily determined from the *in vivo* experimental images. The perivascular reflectance, R_r, was a source of calibration error in previous attempts to measure *in vivo* retinal oxygen saturation.[1,26]

The data obtained from this experimental design provide measures of the spectral behavior of the perivascular retinal reflectance (R_r). Referring to the light-path analysis from Fig. 1, combining and simplifying Eqs. (1) and (4) yields

$$S_1 - S_4 = R_r(\Psi + \Psi_r) - R_r(\Psi T_s T_a + \Psi_r) = R_r \Psi(1 - T_s T_a). \tag{9}$$

When $T_s T_a \ll 1$, as seen when light is highly absorbed by hemoglobin (450–600 nm), [3,27] then Eq. (9) further simplifies,

$$S_1 - S_4 \approx R_r \Psi. \tag{10}$$

Because the power from the light pipe is normalized at each wavelength, the relative reflectance of the perivascular fundus is given by $S_1 - S_4$ at wavelengths significantly absorbed by hemoglobin.

7 Results

The spectra of the measured components, S_1, R_v, and S_4 from a retinal vein are shown in Fig. 2. Each spectrum is a complex combination of the interaction of the source flux Ψ and the reflected flux Ψ_r with a specific region of the retinal anatomy. These signals are similar to the retinal reflectance spectra reported by others.[14] We used the spectra from the 460–521 nm region to calculate the values $-\log(R_v/S_1)$ and $S_1 - S_4$.

Figure 3 shows the spectra of the perivascular retina $[-\log(S_1)]$, an adjacent retinal artery $[-\log(R_v)]$, and the spectra of $-\log(R_v/S_1)$. Fluctuations in power in the two empiric signals are removed by dividing R_v by S_1. Because the reflected flux Ψ_r is an integrated signal from the globe, it contains a bulk average of the arterial, capillary, and venous hemoglobin along with pigment signals from the eye. Dividing R_v by S_1 significantly reduces signal noise (removing Ψ) while shifting the minimum to the right for arteries and to the left for veins (removing Ψ_r).

For the BGO technique to be useful, the analysis must be consistent with changes in vessel diameter, illumination angle, blood concentration, and oxyhemoglobin saturation. Figure 4 shows the monochromatic image of a region of a swine retina at 460 nm. One can see the vessel shadows adjacent to and

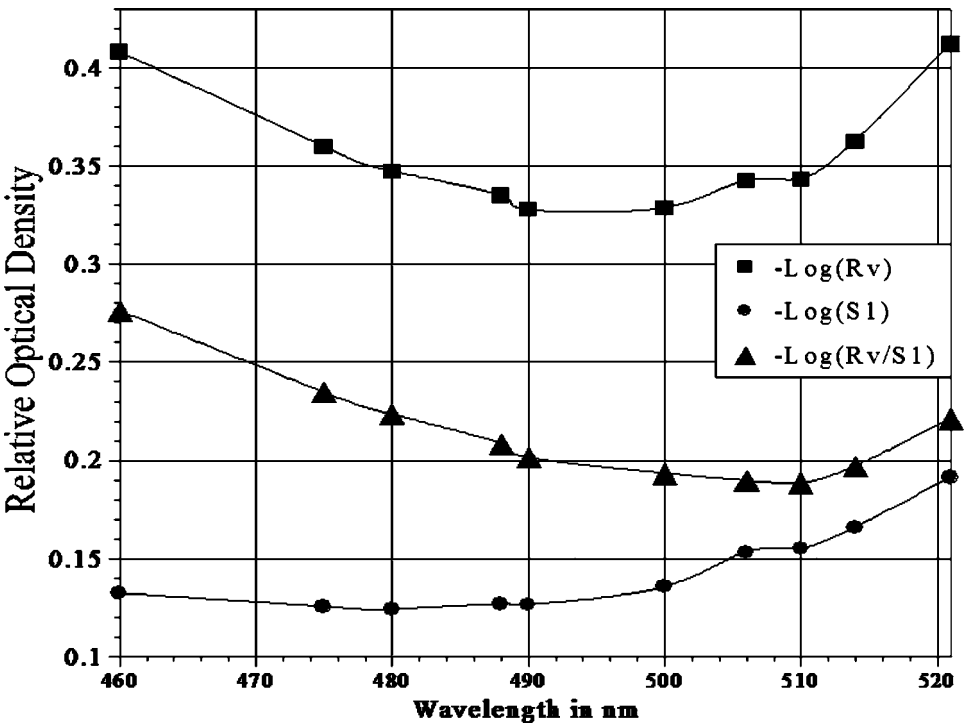

Fig. 3 The spectra shown above were taken from a retinal artery [$-\log(R_v)$] and the adjacent perivascular retina. Note that fluctuations in the power terms seen in these two signals are attenuated when dividing R_v by S_1. The reflected flux Ψ_r is an integrated signal from the globe and has a bulk average of the arterial and venous hemoglobin signals. Dividing R_v by S_1 removes Ψ_r, shifting the minimum to the right for arteries and to the left for veins.

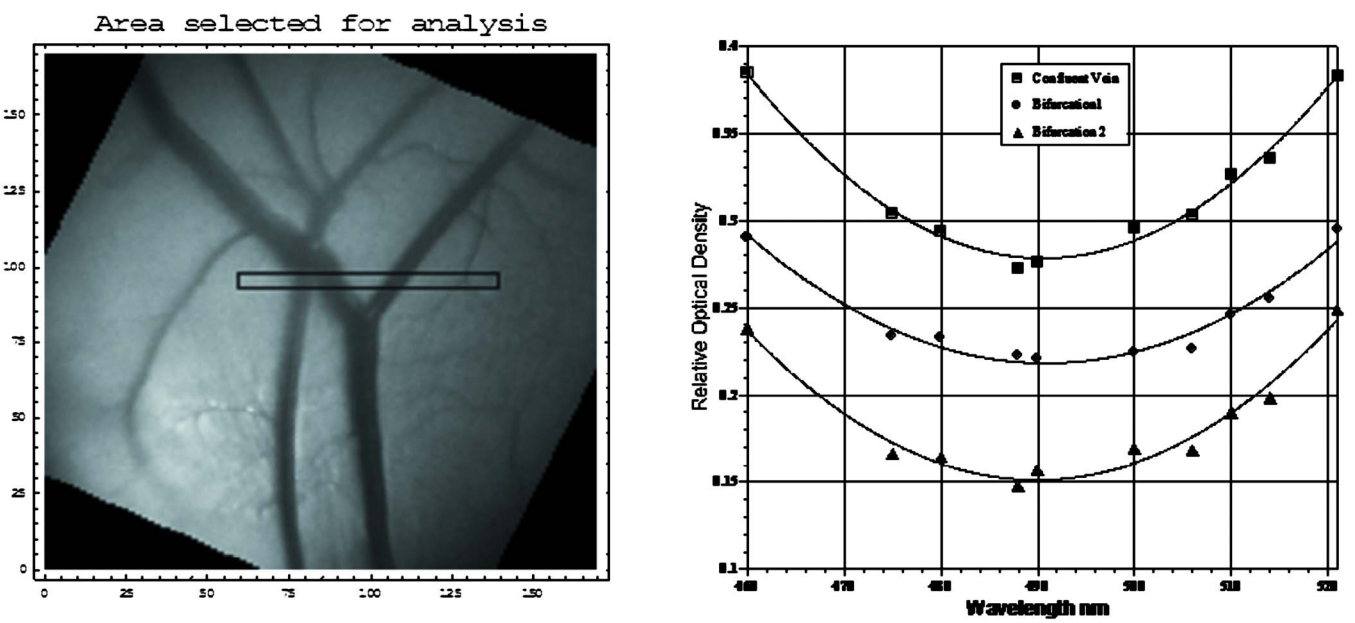

Fig. 4 Shown above is a monochromatic image of the retina at 460 nm that shows the vessel shadows adjacent to and just left of the vessels. The shadow is most apparent where the left-hand bifurcation of the large vein crosses over the artery that is also to the left of the large vein in the image. The minima of the spectra of $-\log(R_v/S_1)$ from the branches of the bifurcated vein and the large confluent vein to the right of the large artery in the image are shown above. Note that the minima are very similar when scans are taken from markedly different sized veins with different angles of illumination.

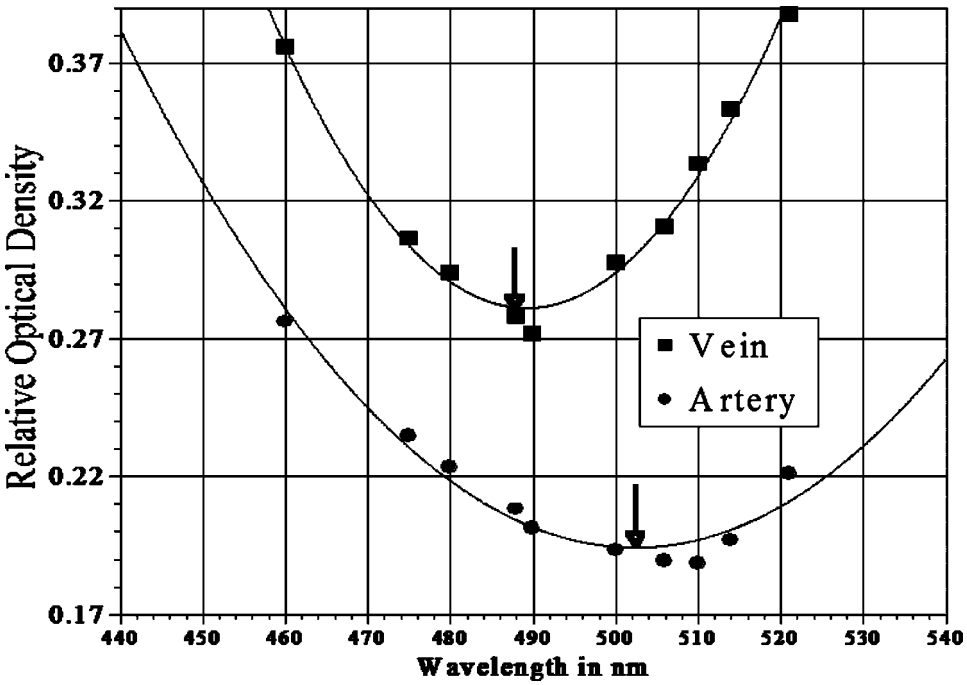

Fig. 5 The spectra of $-\log(R_v/S_1)$ for the artery and vein shown in Fig. 4 are shown here. The artery and vein have minima that are significantly different from each other and behave as predicted by the BGO technique.[2,3]

just left of the vessels. The shadow is most apparent where the left-hand bifurcation of the large vein crosses over the artery that is also to the left of the large vein in the image. The minima of the spectra of $-\log(R_v/S_1)$ from the branches of the bifurcated vein and the large confluent vein to the right of the large artery in the image are also shown in Fig. 4. Local differences in retinal metabolism and autoregulation will cause small variations in the oxyhemoglobin saturation found in two veins that feed a larger vein. The confluent vein should have a bulk average of the two feeder vein oxyhemoglobin saturations. The minima shown in Fig. 4 are very similar when scans are taken from markedly different-sized veins with different angles of illumination and the large vein minimum is between the two feeder vein minima as expected. Figure 5 shows how the spectra of $-\log(R_v/S_1)$ for the artery and the vein shown in Fig. 4 have minima that are significantly different from each other and behave as predicted by the BGO technique.[2,3] The minimum of the arterial fit is 502 nm and the vein is 489 nm, demonstrating sensitivity to oxygen saturation.

In Fig. 6, we show the relative optical density and retinal reflectivity from a swine retinal artery calculated using Eqs. (8) and (10). The BGO minimum shown here is in the region of the spectrum expected for an artery, and the reflectivity of the perivascular fundus is nearly neutral. By selecting the capillary-poor perivascular region and using our light-path analysis to remove the scattered light component Ψ_r, we are able to determine the retinal reflectance (R_r). Because 460–521 nm light that traverses the retinal pigment epithelium is nearly all absorbed by melanin,[14] the return signal R_r, shown in Fig. 6, is nearly all flux that has been scattered back to the detector from the inner retina. This result is consistent with recently published work with a retinal microsurgery isolated *in vivo* inner retina, showing that the perivascular inner retina has very little absorption and is nearly spectrally neutral.[17]

On the basis of these observations, we fit a parabola to the plot of $-\log(R_v/S_1)$ for the retinal arteries in four swine and calculated the minima. A calibration plot was generated by comparing these minima to the oxyhemoglobin saturations in the swine arterial circulation. The quality of the calibration plot was evaluated by calculating the standard deviation of the residuals. Figure 7 shows the calibration plot for this *in vivo* analysis using BGO to analyze 22 measurements in 4 swine with different arterial oxyhemoglobin saturations, vessel diameters (58–130 μm) and hematocrits (24–45%). The slope of 0.33 nm/percent saturation, the intercept of 469 nm and the standard deviation of the calibration residual error of $\pm$3.4% saturation are similar to BGO in hemoglobin and blood.[2,3] The difference in calibration intercepts from the hemoglobin calibration line to the blood calibration line in transmission is related to the slope of wavelength-dependent scattering and is discussed at length elsewhere.[3] The opposite shift in intercepts seen when BGO is used *in vivo* is likely due to the change in the sign of the slope of wavelength-dependent scattering when a signal is collected in reflection in the retina rather than in transmission with a spectrophotometer.[3] Using the calibration line from Fig. 7 to convert minima to saturations, the large vessels shown in Fig. 4 have a retinal venous oxyhemoglobin saturation of 64% (489 nm) and retinal arterial oxyhemoglobin saturation of 98% (502 nm).

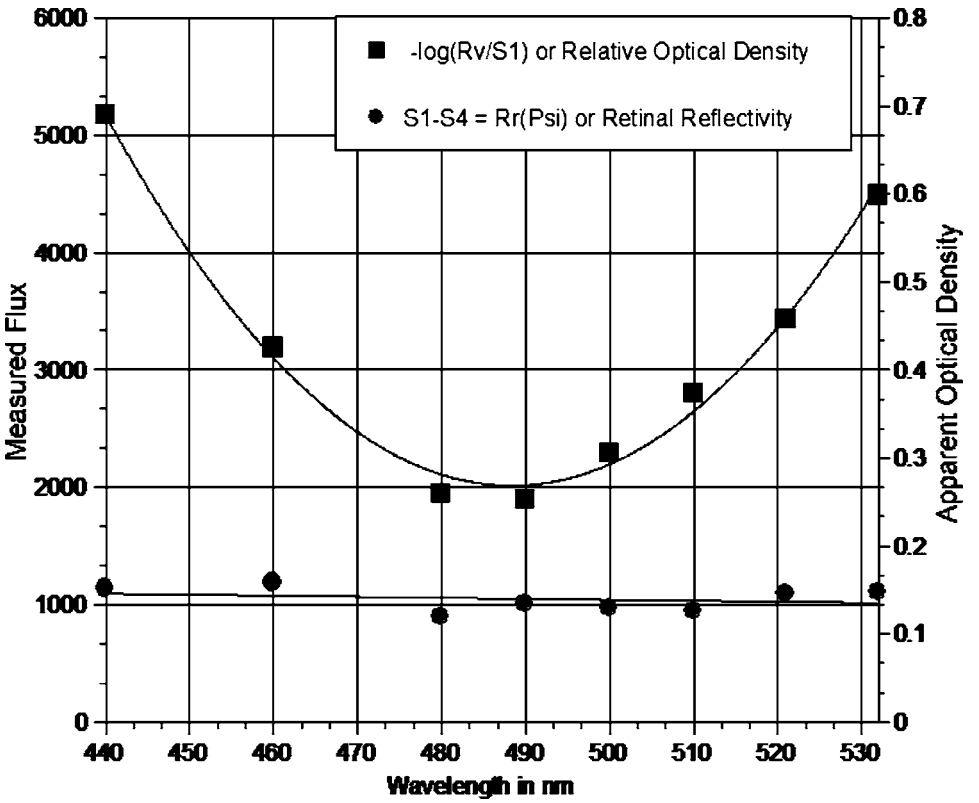

Fig. 6 Shown above are the relative optical density and retinal reflectivity from a swine retinal vein using Eqs. (8) and (10). Note that the minimum is well preserved and the reflectivity of the perivascular fundus is nearly neutral in this region of the spectrum.[17]

8 Spectral Minimum *In Vivo* Error Sensitivity

We performed multiple measures on vessels in the same region moving up one pixel at a time for five lines. The standard deviation of the minima residuals was ± 0.33 nm or 1% saturation ($n=15$). Though this is not exactly the same as repeated measures at the same position, it is a more accurate test of the sensitivity of the method to error because changes in oxyhemoglobin saturation over time and systematic movements are significant confounders likely more important than the changes that occur over a five-pixel range while one frame of data is being collected.

One longstanding problem with retinal oximetry has been the poorly conditioned nature of the equations. Small errors in data lead to far larger errors in the oxygen saturation determinations.[1,28] We evaluated the conditioning of the BGO technique theoretically by assuming a 1% error in each optical density and rereducing the swine reflectance data. A 244-value Gaussian distributed pseudorandom number set with a zero mean and a standard deviation of ± 0.01 was generated. Using the spectra from two swine arterioles and a venule with different oxyhemoglobin saturations (96.7, 85, 54%) and three (475, 488, 514 nm), four (475, 488, 500, 514 nm), five (460, 475, 488, 500, 514 nm) and 10 wavelengths (460, 475, 480, 488, 490, 500, 506, 510, 514, 521 nm), we measured the standard deviation of the calculated minimum when the 244 errors where added to the spectra. The greatest residual error was seen using the 96.7% oxyhemoglobin saturation data with three wavelengths (± 2.7% saturation), and the lowest error when 54% oxyhemoglobin saturation data with 10 wavelengths were used (± 0.9% saturation).

9 Comment on Intravitreal Illumination

Intravitreal illumination is highly invasive, requiring a puncture through the pars plana. It must be performed in a sterile environment by a highly trained practitioner. A vitrectomy is also necessary if one seeks to freely move the light probe through the vitreous chamber. As such, we are not proposing intravitreal illumination as the basis for a widely applicable retinal oximetry test. We do emphasize that the unique light paths provided by intravitreal illumination are particularly useful for developing models of light propagation in the posterior chamber. These model equations take advantage of the reduced specular reflections occurring anterior to the blood column in the vessel and also remove the possibility of light double passing through blood vessels. Using these model equations with information available from other sources allowed us to demonstrate the relative contribution of S_2 (return light through the vessel) and S_3 (backscattered light from the vessel and its contents) to the return signal from the center of the vessel. The analysis using this unique geometry also allowed us to solve for the spectrum of the perivascular inner retina without using Spectralon, as we had previously done.[17]

Because the back-reflected light that traversed the vessel and returned to the detector was shown to be negligible when BGO wavelengths were used, removing double-pass light was

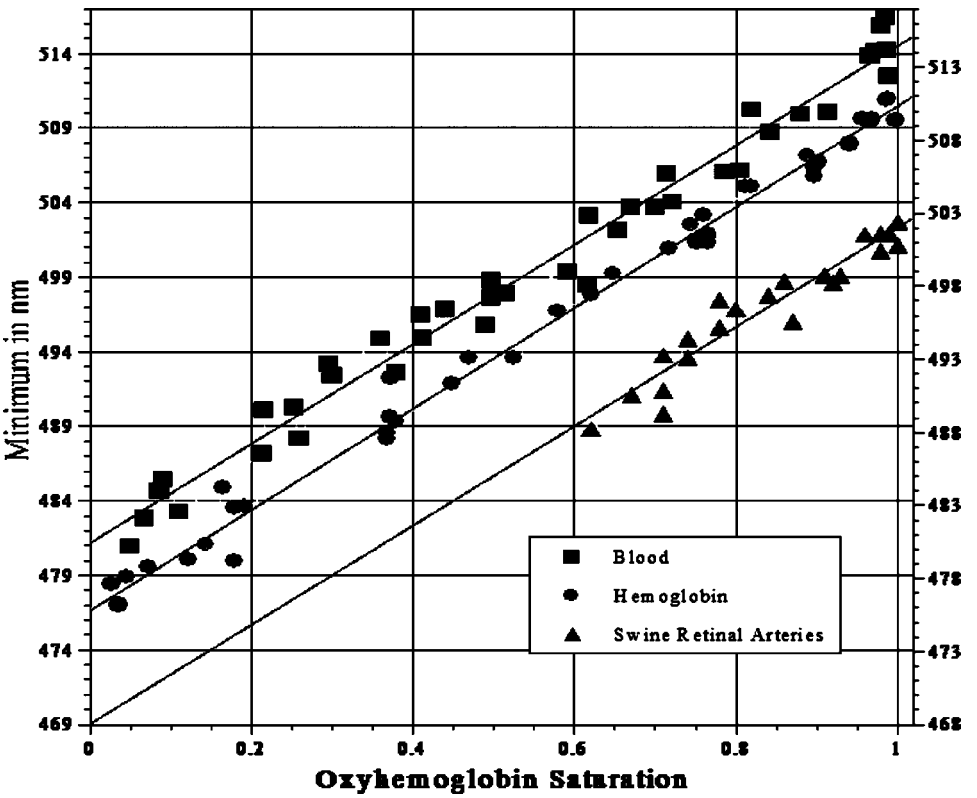

Fig. 7 Shown here are the minima found in the retinal arteries of four swine at multiple different oxygen saturations using a bandwidth of 10 nm. Also shown for comparison are the previously reported minima when a spectrophotometer with a 2-nm bandwidth is used to interrogate blood and hemoglobin in transmission.[2,3] The minima from the veins in Figs. 4 and 6 are all ~489 nm or 64% saturation based on the *in vivo* calibration line above.

shown to be unnecessary. Our work here indicates that the exclusion of central glints or specular reflections from anterior to the vessel remains an issue, but an on axis illumination system that allowed for the removal of the glint would lead to a similar set of model equations.

10 Arterial Calibration of Venous Measurements

The use of arterial signals to calibrate venous measurements using BGO as done here assumes that the arterial profiles and the vein profiles have the same components. The retinal arteries contain blood, are anatomically in analogous circumstances with the same light paths, have vessel walls that scatter light, are in the same size range, and can have the oxyhemoglobin saturation manipulated so that it reaches the range seen in veins. It will be very difficult to generate a better model for the retinal venous circulation than the retinal arteries. However, we know that, aside from oxyhemoglobin saturation, there is a physiologic anemia on the venous side of the circulation, retinal veins are often larger than retinal arteries and venous vessel walls are thinner than corresponding arterial vessel walls. Our results address some of these concerns directly and others by inference.

The sizes and the hematocrits of the blood in the arterial vessels we analyzed varied substantially without causing a significant change in the minima we measured based on these parameters. This makes it unlikely that the differences in size between the arteries and veins or physiologic changes in hematocrit from the arterial to venous circulation will have a significant impact on calibration. We remain uninformed about how different vessel wall thicknesses may influence the backscattered light, but the arterial and venous saturations determined using BGO are reasonable.

11 Conclusions

BGO, described previously in hemoglobin and blood,[2,3] is demonstrated here *in vivo* in an anesthetized pig using a specialized optical system. BGO is sensitive to oxygen saturation and is robust to errors at the 1% level. The relative contribution of single-pass light, double-pass light by inference, and backscattered light in reflectance retinal spectroscopy was separately measured and reported. The shift in BGO calibration line intercepts caused by the slope of wavelength-dependent scattering described by us previously using blood in transmission was present in a system using reflected light, demonstrating a similar but opposite shift in the calibration line intercepts. More work is needed to evaluate varied blood concentration, vessel diameter, blood flow, vessel wall scattering, and techniques for excluding the vessel glints when on axis illumination is used for BGO.

References

1. M. H. Smith, K. R. Denninghoff, A. Lompado, J. B. Woodruff, and L. W. Hillman, "Minimizing the influence of fundus pigmentation on retinal vessel oximetry measurements," *Proc. SPIE* **4245**, 135–145 (2001).

2. K. R. Denninghoff, R. A. Chipman, and L. W. Hillman, "Oxyhemoglobin saturation measurements by green spectral shift," *Opt. Lett.* **31**, 924–926 (2006).
3. K. R. Denninghoff, R. A. Chipman, and L. W. Hillman, "Blood oxyhemoglobin saturation measurements by blue-green spectral shift," *J. Biomed. Opt.* **12**, 034020 (2007).
4. J. B. Hickam, R. Frayser, and J. C. Ross, "A study of retinal venous blood oxygen saturation in human subjects by photographic means," *Circulation* **27**, 375–385 (1963).
5. A. J. Cohen and R. A. Laing, "Multiple-scattering analysis of retinal blood oximetry," *IEEE Trans. Biomed. Eng.* **23**, 391–400 (1976).
6. J. S. Tiedeman, S. E. Kirk, S. Srinivas, and J. M. Beach, "Retinal oxygen consumption during hyperglycemia in patients with diabetes without retinopathy," *Ophthalmology* **105**, 31–36 (1998).
7. F. C. Delori, "Noninvasive technique for oximetry of blood in retinal-vessels," *Appl. Opt.* **27**, 1113–1125 (1988).
8. M. H. Smith, K. R. Denninghoff, L. W. Hillman, and R. A. Chipman, "Oxygen saturation measurements of blood in retinal vessels during blood loss," *J. Biomed. Opt.* **3**, 296–303 (1998).
9. D. Schweitzer, M. Hammer, J. Kraft, E. Thamm, E. Konigsdorffer, and J. Strobel, "*In vivo* measurement of the oxygen saturation of retinal vessels in healthy volunteers," *IEEE Trans. Biomed. Eng.* **46**, 1454–1465 (1999).
10. M. Hammer, E. Thamm, and D. Schweitzer, "A simple algorithm for *in vivo* ocular fundus oximetry compensating for non-haemoglobin absorption and scattering," *Phys. Med. Biol.* **47**, N233–N238 (2002).
11. K. Neff, A. Harris, L. Kagemann, S. Kresovsky, R. Dinn, F. Rivera, and E. Rechtman, "Baseline arterial blood saturation is predictive of venous response to hyperoxia," *Invest. Ophthalmol. Visual Sci.* **45**, e-abstract 2591 (2004).
12. E. Stefansson, G. M. Zoega, G. H. Halldorsson, R. A. Karlsson, T. Eysteinsson, and J. A. Benediktsson, "Spectrophotometric retinal oximetry of retinal arterioles and venules," *Invest. Ophthalmol. Visual Sci.* **45**, e-abstract 2588 (2004).
13. N. M. Anderson and P. Sekelj, "Light-absorbing and scattering properties of non-haemolysed blood," *Phys. Med. Biol.* **12**, 173–184 (1967).
14. F. C. Delori and K. P. Pflibsen, "Spectral reflectance of the human ocular fundus," *Appl. Opt.* **28**, 1061–1077 (1989).
15. A. Lompado, M. H. Smith, L. W. Hiliman, and K. R. Denninghoff, "Multi-spectral confocal laser ophthalmoscope for retinal vessel oximetry," *Proc. SPIE* **3919**, 67–73 (2000).
16. M. H. Smith, K. R. Denninghoff, A. Lompado, J. B. Woodruff, and L. W. Hillman, "Minimizing the influence of fundus pigmentation on retinal vessel oximetry measurements," *Proc. SPIE* **4245**, 135–145 (2001).
17. D. A. Salyer, K. R. Denninghoff, N. Beaudry, S. Basavanthappa, K. Twietmeyer, M. Eskandari, R. I. Park, and R. A. Chipman, "Intravitreal illuminated spectroscopy of the swine fundus using subretinal spectralon," *J. Biomed. Opt.* **13**, 044004 (2008).
18. M. D. Knudtson, B. E. K. Klein, R. Klein, T. Y. Wong, L. D. Hubbard, K. E. Lee, S. M. Meuer, and C. P. Bulla, "Variation associated with measurement of retinal vessel diameters at different points in the pulse cycle," *Br. J. Ophthamol.* **88**, 57–61 (2004).
19. H. C. Chen, V. Patel, J. Wiek, S. M. Rassam, and E. M. Kohner, "Vessel diameter changes during the cardiac cycle," *Eye* **8**, 97–103 (1994).
20. M. J. Dumskyj, S. J. Aldington, C. J. Dore, and E. M. Kohner, "The accurate assessment of changes in retinal vessel diameter using multiple frame electrocardiograph synchronised fundus photography," *Curr. Eye Res.* **15**, 625–632 (1996).
21. G. P. Topulos, N. R. Lipsky, J. L. Lehr, R. A. Rogers, and J. P. Butler, "Fractional changes in lung capillary blood volume and oxygen saturation during the cardiac cycle in rabbits," *J. Appl. Physiol.* **82**, 1668–1676 (1997).
22. Labsphere, "A guide to reflectance coatings and materials," Labsphere Technical Guide (2002).
23. W. M. W. Viola P, "Alignment by maximization of mutual information," *Int. J. Comput. Vis.* **24**(2), 137–154 (1997).
24. M. H. Smith, "Oximetry of blood in retinal vessels," PhD dissertation, Univ. of Alabama, Huntsville (1996).
25. K. R. Denninghoff, M. H. Smith, R. A. Chipman, L. W. Hillman, P. M. Jester, C. E. Hughes, F. Kuhn, and L. W. Rue, "Retinal large vessel oxygen saturations correlate with early blood loss and hypoxia in anesthetized swine," *J. Trauma: Inj., Infect., Crit. Care* **43**, 29–34 (1997).
26. J. M. Beach, K. J. Schweitzer, S. Srinivas, D. Kim, and J. S. Tiedeman, "Oximetry of retinal vessels by dual-wavelength imaging: Calibration and influence of pigmentation," *J. Appl. Physiol.* **86**, 748–758 (1999).
27. W. G. Zijlstra, A. Buursma, and O. W. van Assendelft, *Visible and Near Infrared Absorption Spectra of Human and Animal Haemoglobin: Determination and Applications*, VSP BV, Zeist, The Netherlands (2000).
28. M. H. Smith, K. R. Denninghoff, A. Lompado, and L. W. Hillman, "Effect of multiple light paths on retinal vessel oximetry," *Appl. Opt.* **39**, 1183–1193 (2000).